

## RESEARCH ARTICLE

Ab-initio tiling and atomic structure for decagonal ZnMgDy  
quasicrystal

M. Mihalkovič<sup>†</sup> Institute of Physics, Slovak Academy of Sciences, Dubravská cesta 9,  
84511 Bratislava, Slovakia

J. Richmond-Decker and C. L. Henley, Dept. of Physics, Cornell University, Ithaca NY  
14853-2501 USA

M. Oxborrow, National Physical Lab, Hampton Road Teddington, Middlesex TW11 0LW  
U.K.  
(– –, 2012)

We discover the detailed atomic structure of  $d$ -MgZnY, a stable decagonal quasicrystal alloy of the layered Frank-Kasper type, and related phases, using the “tiling and decoration” approach. The atoms have invariable sites in the rectangle and triangle tiles of a 10-fold-symmetric planar tiling. To discover the lowest-energy structures, we combine the methods of density functional theory (DFT) total energy calculations, empirical oscillating pair potentials (fitted to DFT), fitting effective Hamiltonians for tilings, and discovering optimum tiling structures using a nonlocal tile-reshuffling algorithm. We find a family of practically stable compounds with varying composition, including the decagonal quasicrystal and the known Mg<sub>4</sub>Zn<sub>7</sub> phase these are more stable than competing icosahedral structures by a small margin.

**Keywords:** Frank-Kasper; effective Hamiltonian; Mg-Zn-Y; rectangle-triangle tiling; ab-initio energies

## 1. Introduction

Quasicrystals are grouped into several major classes according to their chemistry and local order, one of which is the “Frank-Kasper” class. In such a structure [1], the atoms are packed such that neighbors always form tetrahedra, and only four shells of neighbors are possible, having coordination numbers CN=12, 14, 15, or 16. The Frank-Kasper structures in the decagonal phase are packings of atoms of two different sizes [14] such that “small” atoms have icosahedral (CN=12) coordinations, “large” atoms occupy the CN=15 or 16 sites, and either kind might occupy the CN=14 sites [2, 3]; the fractional content of  $L$  atoms is typically 35–40%. The same local order is found in well-known icosahedral Frank-Kasper quasicrystals, including stable  $i$ -AlMgZn [4]. In all these systems, (majority) Al/Zn plays the role of the “small” atom, Mg is the “large” atom, and rare earths (RE) are even larger.

Some icosahedral Frank-Kasper quasicrystals are well understood, thanks to the solution of large “approximant” crystals (meaning the unit cell is an exact fragment of the quasicrystal structure, and the lattice parameters have particular relationship to the quasilattice parameters of the quasicrystal). Decagonal FK quasicrystals are

---

<sup>†</sup> Corresponding author. Email: clh@ccmr.cornell.edu

less known; the *stable* ones [5–8, 14] are the (presumably isostructural)  $d$ -ZnMgDy and  $d$ -ZnMgY; the former has composition  $\text{Zn}_{60}\text{Mg}_{38}\text{Dy}_2$  [11]. In general the composition is  $\text{ZnMgRE}$  (where RE=rare earth, specifically Y,Dy,Ho,Er).

The structure was not solved from diffraction, as it was impossible (until recently) to grow large (quasi)crystals [11]; one powder diffraction fit was carried out, using an earlier version of the structure model proposed in this paper [9]. Very recently, preliminary experimental results have been obtained on single (quasi)crystals of decagonal MgZnY [10]. Till recently, the most detailed structural information on  $d$ -MgZnRe was Abe's [8] high-resolution electron microscope (HREM) images. Finally, the following known structure types are all crystalline approximants of the Frank-Kasper decagonal:  $\text{AlMg}_4\text{Zn}_{11}$ ,  $\text{Al}_3\text{Zr}_4$ ,  $\text{Al}_2\text{CuLi}$ , and  $\text{Mg}_4\text{Zn}_7$ .

In the present work, we aim to *predict* the detailed structure of the decagonal phase, ultimately to the point that total energy calculations can confirm the stability of the decagonal with respect to other phases. Such comparisons are notoriously difficult in quasicrystals, since a wrongly occupied (yet rare) site may have negligible effects on diffraction and HREM, yet greatly increases the energy. Since  $d$ -ZnMgRE contains only 2% of the RE, we initially simplify the problem to binary Zn–Mg models. (The binary decagonal is a plausible phase by itself, as it is *almost* stable with respect to competing ZnMg phases.)

Since the structure is decagonal, the structure is quasi-two-dimensional (the lattice parameters from electron microscopy show the period is two atomic layers). We adopt the *tile-decoration* approach to specifying structure models. This means all space is tiled by copies of two (or a few) polygons (the “tiling”), and in turn each kind of polygon contains a set of sites on which atomic species are assigned, analogous to the Wyckoff sites of an ordinary crystal (the “decoration”). This approach has the following advantages:

- (i) Only a few real parameters are needed to specify the atom locations.
- (ii) We divide the structure problem into two stages (decoration and tiling) which are addressed independently.
- (iii) Using various (periodic) tilings coupled with the same decoration, we can construct a large family of “approximant” crystals with closely related structures. Some are realized in nature, and all of them are convenient for numerical calculations of the total energy, etc., which are awkward to set up for an infinite, aperiodic system.

Our starting point is a decoration-type structure model [2] originally formulated using the Penrose or HBS (Hexagon-Boat-Star) tilings, but more naturally based on the rectangle-triangle (RT) tiling.

All our results are based on ab-initio calculations with the VASP package [12], initially in the fitting of pair potentials (Sec. 3) and finally for computing phase stability of the final structures (Sec.4.2).

## 2. Basic atomic structure as tile decoration

The basis of our structure model is that all the low energy structures are tilings of the plane by two kinds of tile, the Triangles (T) and Rectangles (R) shown in Figure 1(a). The main tile edges (heavy lines in Fig.1) have length (on the plane)  $a = 4.52\text{\AA}$ , and are oriented at angles differing by multiples of  $2\pi/10$ . A second kind of edge (dashed lines in the figure). of length  $b \equiv 2a \sin(2\pi/10) \cong 5.31\text{\AA}$  points along directions halfway between the “ $a$ ” edge directions. Each kind of tile always has the same “decoration” by atoms. The three-dimensional structure is formed

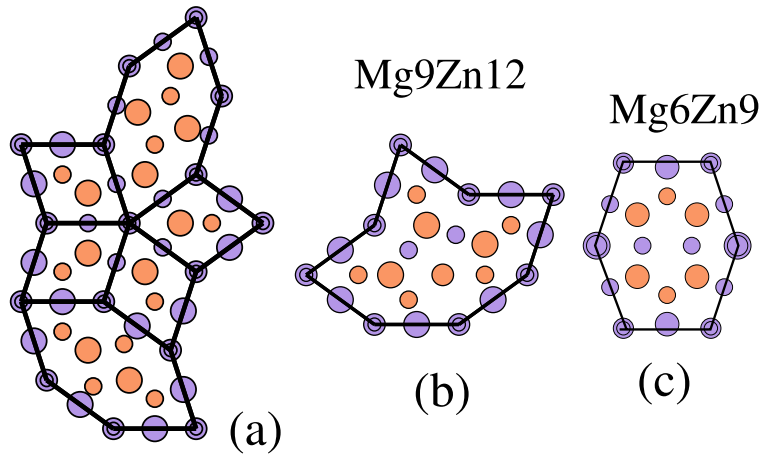


Figure 1. Atomic decoration. Zn atoms are shaded darker. Larger circles are lower in height along (pseudo)decagonal axis. (a). Tiling of Fat Rhombus and Hexagon. Solid (dashed) lines are *a* (*b*) type linkages respectively. The latter divide these into identically decorated Rectangles and Triangles. (b). Boat tile and (c) Lozenge tile are additional kinds of tiles that may be added to the F/H

by repeating the pattern perpendicular to the plane with period  $c = 5.16\text{\AA}$ ; each period contains the equivalent of two atomic layers.

Each tile vertex has a column of small atoms, two per lattice constant ( $\text{ZnZn}$ ), with  $z = \pm 0.25$ . [Coordinates  $z$  are given in multiples of the stacking periodicity  $c = 5.2\text{\AA}$ .] Each mid-edge also has a Zn at  $z = 0$  or  $0.5$  (we will explain shortly how this is decided). Finally, the tile interiors have sites which are all large (Mg) atoms, also at  $z = 0.5$  or  $0$ .

The recipe for the  $z$  heights is simple. Consider all the network of non-vertex atoms: as seen in projection, it consists of one irregular decagon around each vertex, plus one irregular square in the middle of each Rectangle tile. Both polygons have an even number of vertices, so the network is bipartite; we simply assign height 0 to the even vertices and height 0.5 to the odd vertices. This ensures that these atoms form pentagonal antiprisms around all the Zn on vertices. A corollary is that, on either side of an *a* edge, we have Mg atoms at the *same* height, different from that of the mid-edge Zn between them; on either side of a *b* edge, we have Mg atoms at different heights.

The rule for the  $z$  heights can be restated as a *global* pattern: the mid-edge Zn has height  $z = 0$  when the orientation angle of its *a* edge is an *even* multiple of  $2\pi/10$  (as viewed from an even vertex towards an odd vertex) or  $z = 0.5$  when the angle is an *odd* multiple of  $2\pi/10$  angle.

We have three starting points:

- (1) the Roth-Henley model [2] of a hypothetical decagonal structure, which turned out to capture the main motifs in subsequently discovered alloys;
- (2) two known, simple alloy structures are in fact approximants of the decagonal structure.
- (3) The high-resolution electron microscopy (HREM) images of  $\tau$ -ZnMgDy was analyzed to consist largely of Hexagons and Fat Rhombi (see Ref. [15], Figure 1); the same is true for decagonal ZnMgDy, according to our reanalysis of Ref. [16],

Say the Rectangles are surrounded entirely by Triangles (this is favored energetically as explained in Sec. 3). Then the tiles necessarily group into Hexagons (composed of one Rectangle and two Triangles) or Fat Rhombi (two Triangles each). The known approximants  $\text{Zn}_7\text{Mg}_4$  and  $\tau$ -ZnMgDy [15], as well as the HRTEM im-

Table 1. Stoichiometry of the tilings.  $N_{tri}$  and  $iN_{rec}$  are numbers of triangles and rectangles respectively,  $N$  is number of nodes in the unit cell,  $x$  fractional content of the species in the alloy. In the last row,  $\tau=(1+\sqrt{5})/2$

tiling	$N$	$n_{tri}/N$	$n_{rec}/N$	$x_{Zn}$	$x_{Mg}$
triangle	1	1	–	2/3	1/3
rectangle	2	–	1/2	3/7	4/7
$Zn_7Mg_4$	18	1.778	0.111	0.636	0.364
$\tau$ -ZnMgDy	50	1.680	0.160	0.623	0.377
$d$ -ZnMgDy	1	$4\tau^{-2}=1.528$	$\tau^{-3}=0.236$	0.603	0.396

ages of the decagonal phase [see Figure 3(c)], are indeed built from these larger tiles. In the decagonal case (both in the experimental images and also as we predict in Sec. 4), the FatRhombi occur mostly in groups of five forming a Star. Thus, our tiling is built from two out of three tiles from the well-known Hexagon-Boat-Star tiling; therefore we also checked the possibility of allowing a Boat tile (as done in [2]). This first required testing several plausible candidates for the decoration, of which Fig. 1(b)] was the best energetically, however it still costs about 0.1 eV per Boat tile compared to a pure Rectangle-Triangle tiling using the same atoms. Another alternative tile that can be mixed with Rectangles and Triangles is the “Lozenge” shape [Fig. 1(c) shows the least costly decoration], but that was also determined to cost at least 0.2 eV per Lozenge tile. Consequently, we did not pursue these alternative decorations further.

Given these decoration rules, the R–T tilings are in one-to-one correspondence with a class of atomic structures including approximants and quasicrystals. The decagonal phase forms upon annealing of metastable ternary  $Zn_7Mg_4$  structure, and the  $\tau$ -approximant is a transitional state [15]. Table 1 summarizes the stoichiometry of the tilings assuming a purely binary ZnMg decoration rule.

### 3. Fitting the tile Hamiltonian

It is feasible to obtain ab-initio relaxed energies of the decoration structures from relatively small R-T tilings, but not for an exhaustive enumeration of them. Hence we pursued an effective Hamiltonian approach, consisting of two stages (i) from ab-initio energies to an interatomic pair potential (ii) from the pair potential to a “tile Hamiltonian” depending only on the tile degrees of freedom.

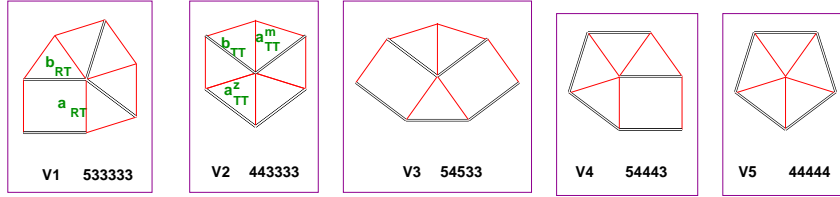
In the first stage, “empirical oscillating” pair potentials (EOPP) [17], were fitted to a database of 7617 samples for ab-initio forces (at  $T > 0$ ) and 48 energy differences (for  $T = 0$  relaxed structures) calculated using VASP [12], and extended to ternaries including Y; when a promising structure from pair-potential and/or tile-Hamiltonian optimization was checked by ab-initio, the results were fed back into the database. The oscillations depend on the Fermi wavevector so such potentials are valid only for a fixed conduction electron density; however that means a wide composition range in the present material since all constituents have an effective valence +2.

The potentials have minima at  $3.3\text{\AA}$  [for  $V_{Mg-Mg}(r)$ ] or  $2.9\text{\AA}$  for  $V_{Mg-Zn}(r)$ , while  $V_{Zn-Zn}(r)$  has only a shoulder at the nearest-neighbor distance. The Zn–Zn potential has a strong second-neighbor well at  $4.5\text{\AA}$ , while the other two potentials have humps at  $\sim 1.25$  times the nearest-neighbor distance.

Till now, it has been unclear whether the oscillations in the pair potentials are essential for quasicrystal order in the FK class of alloys. A positive hint is that both the Al-TM and FK classes are believed to be stabilized by the “Hume-Rothery” mechanism [18]: that means that (within the nearly free electron picture) the ions arrange themselves so that the potential seen by electrons has prominent scattering

Figure 2. The five vertex types (out of 10 possible) appearing in rectangle-triangle tilings that optimize the tile Hamiltonian. The “ $a$ ” edges are shown by straight lines (red online) and the “ $b$ ” edges by double lines. Vertex labels are strings of numbers  $\alpha_i$ , where  $\{\alpha_i(\pi/10)\}$  are the corner angles around the vertex.

Edge types are also marked, e.g.  $a_{RT}$  ( $a$  edge shared between a rectangle and a triangle) Note the distinction of  $a_{TT}^m$  (mirror edge) and  $a_{TT}^z$  (“zigzag” edge, twofold axis at its midpoint).



at wavevectors that span the Fermi surface, thereby mixing electronic states near the Fermi energy so as to create a pseudogap there and lower the energy of the occupied states. Expressed in terms of the real-space structure, this is equivalent to saying the pair potentials have strong (“Friedel”) oscillations and that their second or third wells play a role in selecting the structure. Indeed, the second potential wells were shown to be crucial in the Al-TM case [19, 20].

### 3.1. Tile Hamiltonian form and fits

The tile-Hamiltonian approach[25] posits that the stronger interatomic interactions favour the atoms to organize into a decorated tiling (in our case the T/R tiling) which are practically degenerate. The terms of the Hamiltonian that distinguish different tilings are weak enough to be treated as a perturbation. We can collect these contributions and attribute them to the tiling geometry, thus defining a “tile Hamiltonian” acting on these reduced degrees of freedom (which correspond one-to-one to the possible low energy atomic configurations). The tile Hamiltonian’s low-energy states will define a “low-temperature” subensemble, as analyzed below in Sec. 4, which might be built from “super-tiles” which are clusters of the basic tiles.

We consider three possible kinds of terms in  $\mathcal{H}_{\text{tile}}$ :

- Single-tile terms,  $E_R N_R + E_T N_T$ , where  $N_R$  ( $N_T$ ) is the total number of rectangles (triangles). Note that, with the decoration we are using, there is a linear relationship between  $(N_R, N_T)$  and the atom counts  $(N_{\text{Mg}}, N_{\text{Zn}})$ , so this term is equivalent to chemical potentials coupling to the atom numbers.
- Tile-pair “edge” terms, such as  $E(b_{RR})N(b_{RR})$ , for each of the seven possible edge types. Note there are four linear dependences among the counts of these edges and  $(N_R, N_T)$ , e.g.  $2N_R = 2N(a_{RR}) + N(a_{RT})$ : this simply expresses the fact that every rectangle has two  $a$  edges, each shared with either another rectangle or a triangle.
- “Vertex” terms, such as  $E(V_\beta)N(V_\beta)$ , where  $N(V_\beta)$  is the number of one of the ten vertex types (of which five are shown in Figure 2. There are additional linear dependences among the counts of these vertices, most strikingly  $N(\langle 54533 \rangle) = N(\langle 44444 \rangle)$ .

We resolved the ambiguities by using edge terms rather than vertex terms where possible, and making coefficients positive; this choice gives the parametrization of Table 2 For the fit, we used the pair-potential energies from a database of 155 R-T tilings with 29, 44, or 47 vertices, each decorated with atoms and relaxed. The fit results are shown in Table 2. After the single-tile energies, the largest terms were edge energies for  $a_{RR}$ ,  $b_{RR}$ , and  $a_{RT}^z$ ; two smaller “vertex” energies are corrections

Table 2. Fitted energies for terms in tile Hamiltonian (eV)

Object	R	T	$a_{RR}$	$b_{RR}$	$a_{TT}^z$	$V_T$	$V_5$
Energy (eV)	-0.899	-0.620	0.134	0.102	0.030(?)	0.014	0.018

to the edge terms, tending to disfavor vertices  $\langle 433433 \rangle$  and  $\langle 55555 \rangle$ , which we shall call  $V_T$  and  $V_5$  for short.

The reason that rectangle-rectangle terms are so costly is that the large (Mg) atoms in the Rectangle interior are too tightly packed, which can be relaxed by outward displacements only when they adjoin Triangle tiles.

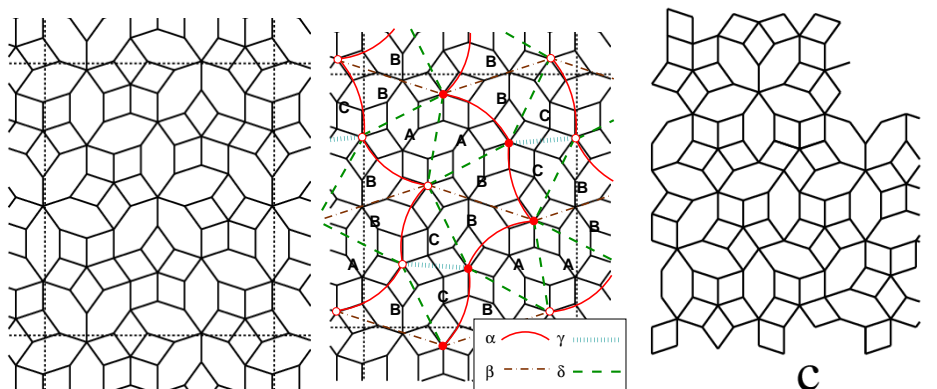
We will see (in Sec. 4) that in the optimum tilings there are no R-R edges at all and no  $V_T$  vertices, furthermore the number of  $V_T$  vertices is constrained so this term breaks no degeneracies. Consequently, *the key interaction is the “zigzag” energy  $E_z$*  (for  $z_{TT}^z$  type edges). This represents the change in the energy of two triangles adjoining along an  $a$  edge, when one is flipped so as to change from mirror symmetry to twofold symmetry around the edge midpoint. But the unrelaxed position of the adjacent Mg atoms is on the edge bisector and thus all nearest-neighbor interactions are unchanged by such a flip! In order to identify the origin of  $E_z$ , we repeated the potential fits using both relaxed and unrelaxed positions, for both the oscillating potentials and a version cut off at  $r = 4.0\text{\AA}$  (so as to have only nearest-neighbor interactions). We found that an  $E_z$  term *can* be generated even with nearest-neighbor interactions, since the mid-edge Zn atom is able to relax along the edge in the mirror-symmetric configuration but is fixed by symmetry to the midpoint in the zigzag (two-fold configuration). However, it appears that the actual  $E_z$  is mainly due to the second-well interaction of the mid-edge Zn atoms on the far sides of each Triangle: the flip changes their separation from a distance  $(\tau/2)b \approx 4.3\text{\AA}$ , close to the second Zn-Zn well at  $4.5\text{\AA}$ , to  $b \approx 5.3\text{\AA}$ , close to a potential maximum at  $5.7\text{\AA}$ .

Incidentally, if two Fat Rhombi adjoin so as to be parallel – a local pattern inimical to most kinds of quasicrystal order – they form a zigzag edge. Thus, in disfavoring that edge the tile Hamiltonian *tends* to favor quasicrystal-like states with fivefold statistical symmetry and long range order, but not in the absolute way that a matching rule does.

### 3.2. Placement of rare earth Y in the ternary

The experimental quasicrystal phase [5–7, 11] is stabilized by a just a few percent of Y atoms, which are known to be effectively even larger than Mg, and (we expect) are filling special favorable sites. Since Y has a larger radius, presumably these are a subset of the largest coordination (CN=16) Mg sites, which are those in Triangles. Due to pair interactions, it turns out, a Rectangle adjoining (by the  $a$  edge) favors Y, thus the most favorable site has Rectangles adjoining on *both* sides, which happens in the “4” corner of the  $\langle 54533 \rangle$  vertex; in fivefold symmetry, these are a fraction  $0.5\tau^{-5}(\tau + 1/4) \approx 8.42\%$  of all Mg sites. However, the Y–Y interaction has a shoulder at  $r \approx 5\text{\AA}$ , so it is disfavorable to have Y atoms separated by the layer spacing  $c$ . Hence, we predict that in MgZnY there is a (global or local) period-doubling with one column of alternating Mg/Y occupancy for each  $\langle 54533 \rangle$  vertex. The final conclusion is a net Y content of 1.4% atomic, which is exactly the experimental observation [11].

Figure 3. (a) Low temperature tiling of the 76-node approximant obtained by Monte-Carlo annealing. Only  $a$  edges are shown in these plots. (The atom content would be  $Mg_{94}Zn_{203}$ .) (b) Supertiling. Its nodes are centers of Stars of five Fat Rhombi; even and odd nodes are marked by closed or open circles. Four kinds of edges (right) are indicated by different lines, and form three kinds of triangular tiles called A, B, or C. (c) Experimental tiling of decagonal ZnMgDy, redrawn from HREM image of Ref. [16].



#### 4. Results: minimum energy tilings

Having obtained the tile Hamiltonian, the next task is to discover (and characterize) which tilings minimize it, by Monte Carlo simulations in medium and large cells. This is far more challenging technically than for tilings of Penrose rhombi, or of Hexagon/Boat/Star tiles, in which any tiling can be accessed from another via a string of *local* reshufflings involving two or three tiles. In the case of the R-T tiling, a nonlocal move called a “zipper” is necessary, encompassing a chain two tiles wide (and typically recrossing itself) that continues until the chain reaches the starting point and closes on itself. [21–23]. The implementation for the R-T case [22, 23] is similar to that for the 12-fold symmetric square-triangle tiling [21], but more complex.

The resulting tilings show a great deal of local order [see the example in Fig. 3(a)]. Some of the order can be understood immediately from the tile Hamiltonian. Most obviously, there are *no* rectangles adjoining by either kind of edge, as expected since those edges are very costly. An immediate geometric consequence is that the rectangles and triangles always combine into Fat Rhombi or Hexagons (as in Figure 1). We also find that only five of the ten vertex types appear (Figure 2); three of the absent vertices are obvious, as they included adjoining Rectangles.

Given there are no R-R edges, the counts of most kinds of edge are constrained through *sum rules* that follow from obvious facts: e.g., every rectangle  $b$  edge has a triangle on the other side, and every triangle  $b$  edge not adjoining a rectangle must be of  $b_{TT}$  type, adjoining another triangle. However, the sum rules do not distinguish the mirror-symmetric ( $a_{TT}^m$ ) or twofold (“zigzag”,  $a_{TT}^z$ ) triangle-triangle edges. Thus, the only remaining term is the “zigzag” cost  $E_z$ : *our ensemble has no numerical parameters* and is defined by minimizing (subject to the other constraints) the number of zigzags (they cannot all be eliminated).

##### 4.1. Supertiling description

A salient motif of the emergent ensemble is that all Fat Rhombi occur in groups of five with a common tip, forming Star tiles. Indeed, a *supertiling* [Fig. 3(b)] is defined, in the in the best-ordered regions of our simulated tilings, by the Star centers (which we shall call “nodes”). Neighboring nodes are related by four kinds of “linkage” denoted  $\alpha$ ,  $\beta$ ,  $\gamma$ , and  $\delta$ . These in turn form edges of three kinds

of tiles, called A, B, and C (see Figure 3(b); B and C tiles necessarily occur in pairs. The numbers of each kind,  $N_A$ ,  $N_B$ , and  $N_C$ , in a given unit cell (or in a case of true decagonal symmetry) are completely determined because (1) the number of rectangles and triangles is determined by the cell, and each supertile is always decorated by the same pattern of the smaller Rectangle/Triangle tiles. (2) considering  $\alpha$  edges shows that  $N_B = N_A + N_C$ . It follows that the frequency of each vertex type is also determined. The *smallest* periodic cell allowed with these tiles has 38 R-T nodes [half the size of Fig. 3(a)].

We have not yet constructed quasiperiodic supertilings, or periodic ones larger than Fig. 3(a), but we conjecture that these exist, and indeed that an ensemble of random tilings is possible. Due to the exceptional asymmetry of these tiles, however, the packing is constrained to an unusual degree, indicating a long correlation range and low entropy for that ensemble. (Only linages  $\alpha$  and  $\beta$  lie in such symmetry directions; all previously known supertilings, e.g. Ref. [27], used linkages in high-symmetry directions, usually the  $a$  or  $b$  vector multiplied by some power of the golden ratio.)

We also have strong reason to believe that R-T tilings made by decorating this supertiling have the lowest possible number of “zigzag”  $a$  bonds (zigzags occur in one chain of four bonds per  $C_2$  tile pair). Thus, the supertiling structures are the ground states of our tile Hamiltonian, and are very nearly degenerate with each other.

The only known quasiperiodic rectangle-triangle tiling is Cockayne’s iterative construction [24]. Like our tiling, that one is entirely built from Fat Rhombi and Hexagons, and it uses the same five vertex types in Fig. 2); however, it has few Stars of five Fat Rhombi, and it has a higher density of zigzag edges.

#### 4.2. Crystallographic consequences and energetic stability

The fact that the Rectangle/Triangle tiling groups into Hexagons and Stars has an important consequence for the atomic structure: following the rule for heights  $z = 0$  or  $0.5$  stated in Sec. 2, all mid-edge Zn atoms on the borders of Hexagons or Stars have the same height, globally; the only mid-edge Zn at the other height are those decorating the five edges around each Star center. (That also explains why Y atoms are observed only in at one height.)

In the minimum-energy tilings, the Y sites (Sec. 3.2) sit in tips of Fat Rhombi that stick in between two Hexagons. This pattern is always part of a decagon, consisting of a Hexagon plus three Fat Rhombi, that would be a regular decagon except that one vertex is “dented” inwards. The Y sites constitute the centers of all these dented decagons, and (for the same reason as the mid-edge Zn sites) all have the same  $z$  value. These two facts have been observed for the Y sites in preliminary refinements of single-crystal data [10].

Experimentally, the phase stability around the composition  $Mg_{40}Zn_{60}$  at low  $T$  is poorly studied, due to diverging equilibration times and further impeded by the low melting point of Mg, and because the low formation enthalpy of the  $MgZn_2$  Laves phase overshadows all other phases at low  $T$ .

*The  $Mg_4Zn_7$  phase [?] is the stable one [26] in our composition range (practically on the tie-line at  $T = 0$ , according to ab-initio calculations).*

The addition of Y is found to make the quasicrystal or approximant structures *stable* with respect to competing phases. This may be attributed to two things (1) a quite strong nearest neighbor Zn-Y attraction (2) the poor fit of Y in substituting into competing structures.

## 5. Discussion

In conclusion, we have reported a realistic study of structural stability and energetics at low temperature of the binary decagonal quasicrystal  $d$ -MgZn, and crystal structures that approximate it, and of the ternary  $d$ -MgZnY. The binary  $d$ -MgZn quasicrystal, which was slightly unstable (according to ab-initio calculations), was stabilized by the inclusion of a small number of Y atoms, as they substitute easily in certain kinds of Mg sites, but are less easily accommodated in the simpler Laves structure that is competing for stability.

We computed the relaxed energy for every tiling in an enumeration of medium-sized tilings (using pair potentials) and then, by numerical fitting, re-expressed the total energies in terms of a “tiling Hamiltonian” with single-tile energies as well as tile-tile interactions [25].

Due to the large cost of adjoining rectangles, our tiling is further constrained to consist of Fat Rhombi and Hexagons (which are respectively combinations of two T tiles, or of two T’s plus one R); this simplifies the optimization so much that there are essentially no free parameters in the effective Hamiltonian, and the resulting tiling satisfies highly constraining local rules.

Since Dy atoms are magnetic, our structure determination also opens a door to accurate modeling of the antiferromagnetism [28] in these materials. The RE sites we propose form a network with nearest-neighbor spacing  $\tau b \approx 8.6\text{\AA}$ . It contains many pentagons, so it is non-bipartite and (assuming the RKKY interaction at that distance is antiferromagnetic) is frustrated.

Highly ordered *icosahedral* [13] quasicrystals are long known in the ZnMgRE system, too. (with composition  $\text{Zn}_{64}\text{Mg}_{27}\text{Y}_9$ [8], for example). Now that the RE site has been identified, it would be of interest to explain how RE stabilizes those structures, and to examine the exact real-space structure.

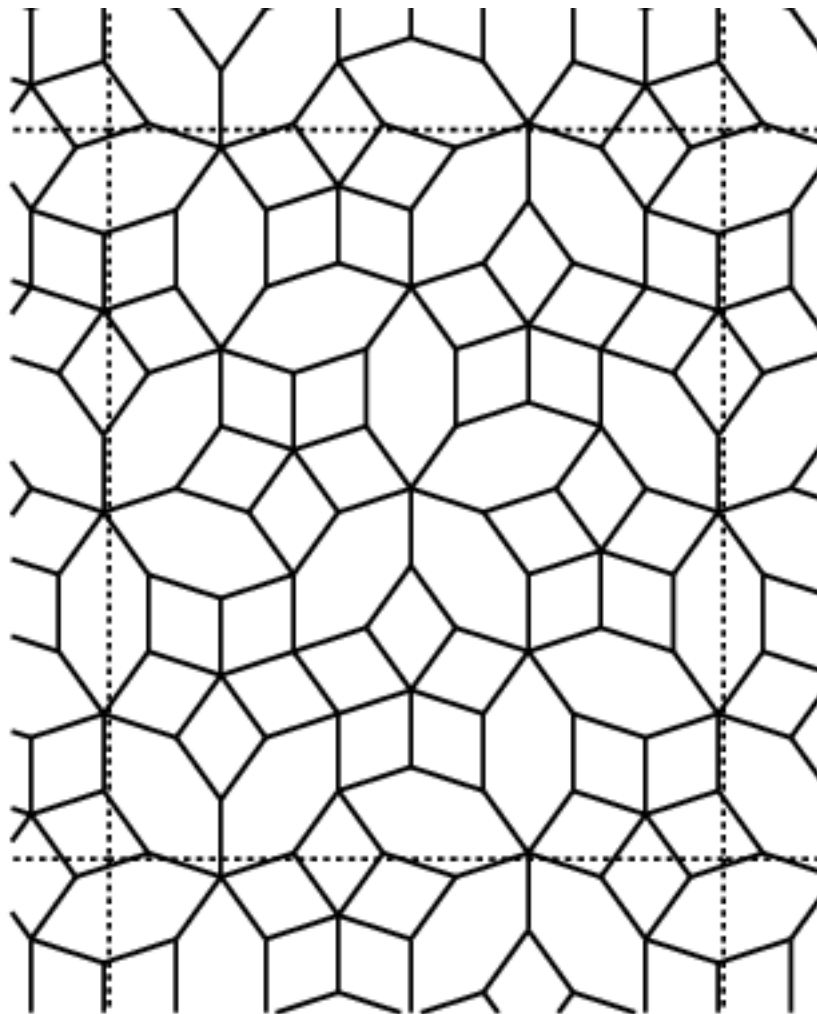
### 5.1. Acknowledgements

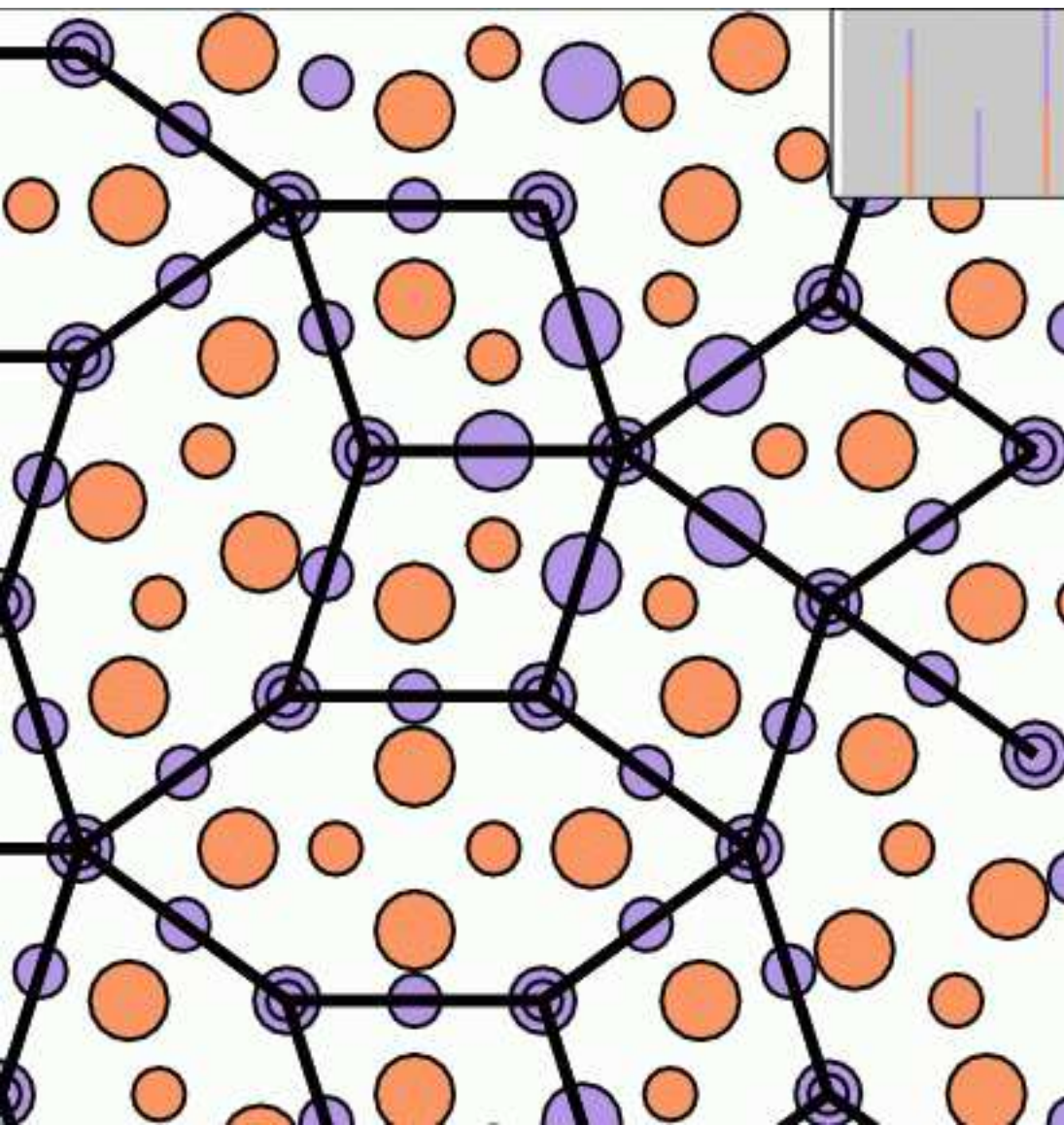
MM, CLH, and J. R-D. by U.S. Dept. of Energy grant DE-FG02-89ER-45405. MM has been also supported by Slovak national grants VEGA j2/0111/11 and APVV-0647-10.

## References

- [1] F.C. Frank and J. S. Kasper, Acta Crystallogr. 11, 184 (1958); *ibid.* 12, 483 (1958).
- [2] J. Roth and C. L. Henley, Phil. Mag. A **75**, 861 (1997).
- [3] M. Mihalkovič and M. Widom, MRS Proceedings 805, LL2.3 (2003).
- [4] T. Takeuchi and U. Mizutani, Phys. Rev. B **52**, 9300 (1995).
- [5] A. Niikura, A. P. Tsai, A. Inoue, and T. Masumoto, Phil Mag Lett 69, 351 (1994). TSAI AP; INOUE A; et al.
- [6] A. P. Tsai, A. Niikura, A. Inoue, T. Masumoto, Y. Nishida, K. Tsuda, and M. Tanaka, Phil. Mag. Lett 70, 169 (1994)
- [7] E. Abe, T. J. Sato, and A. P. Tsai Phil. Mag. Lett. **77**, 205 (1998)
- [8] E. Abe and A. P. Tsai, Phys. Rev. Lett. **83**, 753 (1999).
- [9] R. Sterzel, E. Dahlmann, W. Assmus, K. Saitoh, H. Fuess, M. Mihalkovic and J.-B. Suck, Phil. Mag. Letters, 82, 235 (2002).
- [10] T. Örs and W. Steurer, personal communication.
- [11] T. Örs and W. Steurer, Phil. Mag. 91, 2466 (2011)
- [12] (a) G. Kresse and J. Hafner, Phys. Rev. B, 47, R558 (1993); (b) G. Kresse and J. Furthmuller, Phys. Rev. B 54, 11169 (1996).
- [13] A. P. Tsai, A. Niikura, A. Inoue, A. Masumoto, Y. Nishida, K. Tsuda, and M. Tanaka, Phil. Mag. Lett. **70**, 169 (1994).
- [14] T. J. Sato, E. Abe, and A. P. Tsai, Phil. Mag. Lett. **77**, 213 (1998).
- [15] E. Abe and A. P. Tsai, Acta Cryst. B **56**, 915 (2000).
- [16] E. Abe, T. J. Sato, and A. P. Tsai, Phys. Rev. Lett. **82**, 5269 (1999).

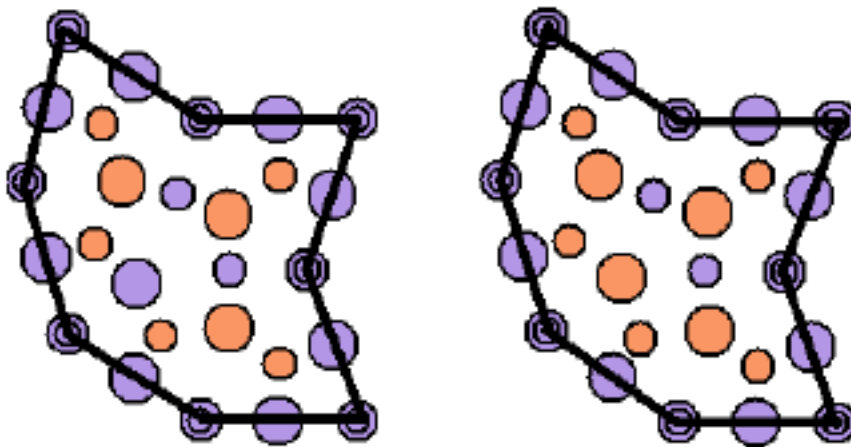
- [17] M. Mihalkovič and C. L. Henley, preprint (arXiv:1109.6931), “Empirical oscillating potentials for alloys from ab-initio fits, and the prediction of quasicrystal-related structures in the Al-Cu-Sc system”
- [18] J. Friedel, *Helv. Physica Acta* 61, 538 (1988).
- [19] S. Lim, M. Mihalkovič, and C. L. Henley, *Philos. Mag.* 88, 1977-1984 (2008).
- [20] S. Lim, M. Mihalkovič, and C. L. Henley, *Z. Kristallogr.* 223, 843-846 (2008).
- [21] M. Oxborrow and C. L. Henley, *Phys. Rev. B* 48, 6966-6998 (1993).
- [22] M. Oxborrow and M. Mihalkovič, in *Aperiodic '94, Proceedings of the International Conference on Aperiodic Crystals*, edited by G. Chapuis and W. Paciorek (World Scientific, 1995), p. 178.
- [23] M. Oxborrow and M. Mihalkovič, in *Aperiodic 97, Proceedings of the International Conference on Aperiodic Crystals*, edited by M. de Boissieu, J.-L. Verger-Gaugry, and R. Currat (World Scientific, 1998), p. 451.
- [24] E. Cockayne, *Phys. Rev. B* 51, 14958 (1995).
- [25] M. Mihalkovič, W.-J. Zhu, C. L. Henley, and M. Oxborrow, *Phys. Rev. B* 53, 9002 (1996).
- [26] H. Okamoto, *J. Phase Equilib.* 15 (1994) 129-130.
- [27] M. Mihalkovič, I. Al-Lehyani, E. Cockayne, C. L. Henley, N. Moghadam, J. A. Moriarty, Y. Wang, and M. Widom, *Phys. Rev. B* 65, 104205 (2002).
- [28] T. J. Sato, H. Takakura, J. Guo, A. P. Tsai, and K. Ohoyama, *J. All. Compounds* 342, 365-8 (2002).
- [29] P. J. Steinhardt, H.-C. Jeong, K. Saitoh, M. Tanaka, E. Abe, and A. P. Tsai, *Nature* 396, 55 (1998).
- [30] M. Mihalkovič, C. L. Henley, and M. Widom, *Philos. Mag.* 91, 2557-2566 (2011).



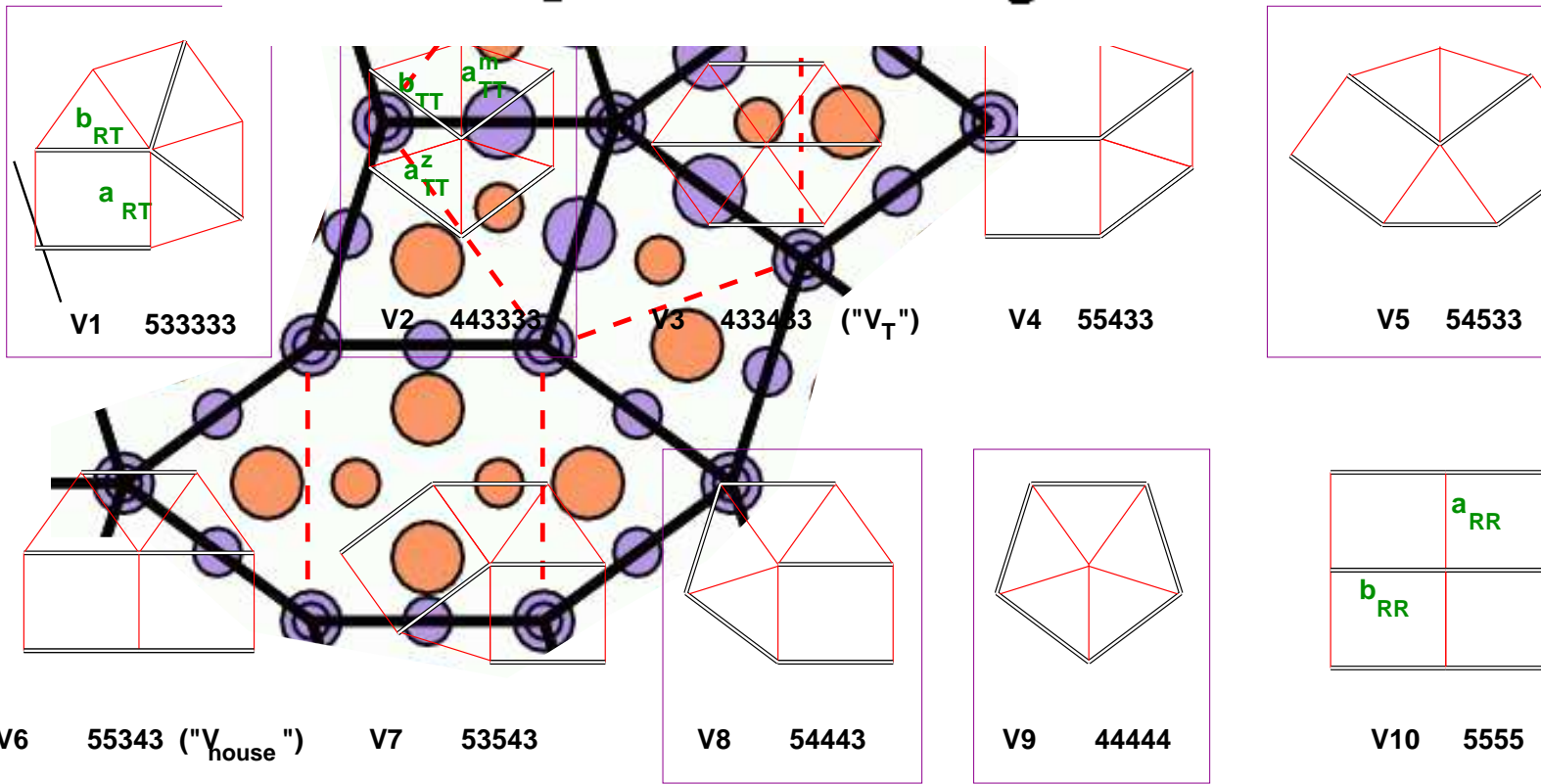


$Mg_8Zn_{13}$

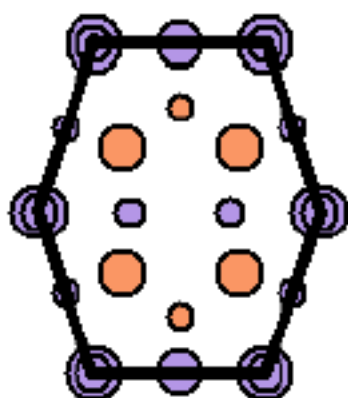
$Mg_9Zn_{12}$



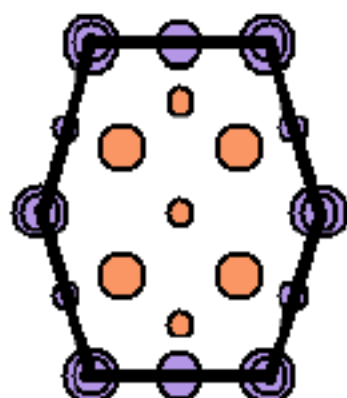
short edge (a):

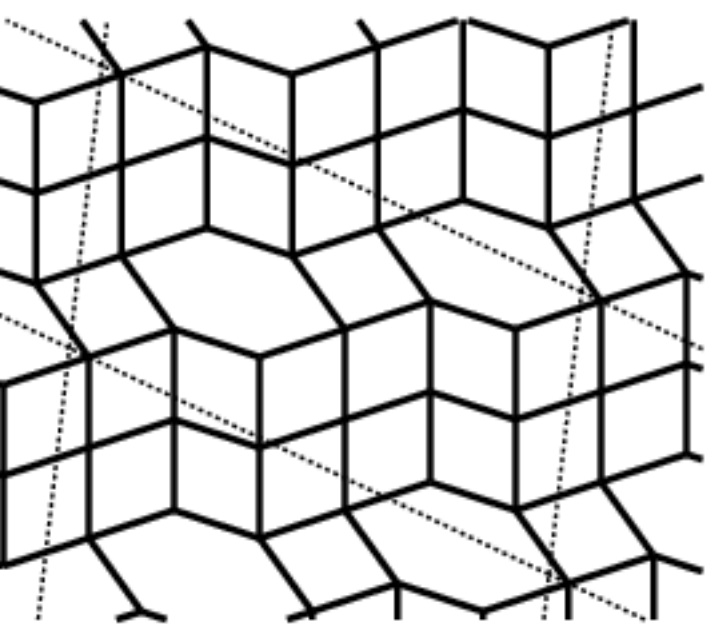


**Mg<sub>6</sub>Zn<sub>9</sub>**

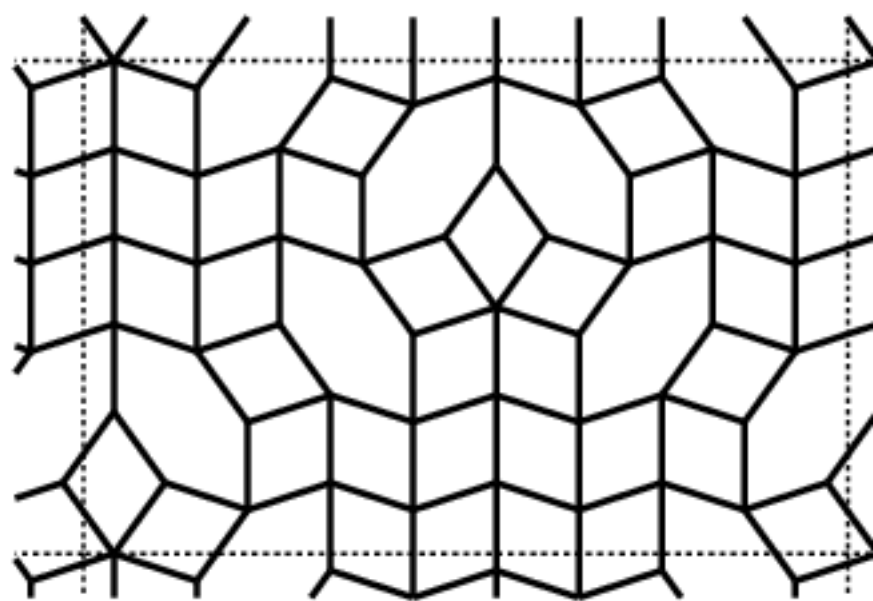


**Mg<sub>7</sub>Zn<sub>7</sub>**





**a**



**b**

